Transverse-Longitudinal Structure Registration and Vibration Measurement via Optical Coherence Tomography

Brian L. Frost,[1, a)] C. Elliott Strimbu,[2, b)] and Elizabeth S. Olson[2, 3, c)]

[1)] *Department of Electrical Engineering, Columbia University, New York, NY, USA*
[2)] *Department of Otolaryngology Head and Neck Surgery, Columbia University, New York, NY, USA*
[3)] *Department of Biomedical Engineering, Columbia University, New York, NY, USA*

[a)] *Corresponding author: b.frost@columbia.edu*
[b)] *Electronic mail: ces2243@cumc.columbia.edu*
[c)] *Electronic mail: eao2004@columbia.edu*

Abstract. Intra-organ of Corti displacement measurements made via optical coherence tomography have provided significant information about cochlear micromechanics in recent years. However, several ambiguities inherent to this modality have complicated interpretation of these measurements. For one, optical coherence tomography measures the one-dimensional projection onto the optical axis of a three-dimensional motion. Also, the optical axis may make a substantial angle with the basilar membrane normal, meaning that structures along the optic axis, measured in a single measurement, may lie in different tonotopic cross-sections. We have developed a method that accounts for both of these ambiguities, to reconstruct the two-dimensional longitudinal-transverse components of displacements of structures within the organ of Corti. This is performed by taking data at multiple longitudinal positions at two viewing angles, without any *a priori* knowledge of the measurement locations or viewing angles. We present a sample data set in which we have applied this program to reconstruct the transverse-longitudinal motion of the base of the outer hair cells in the base of the sensitive gerbil cochlea. The results reinforce the importance of accounting for viewing angle when analyzing and reporting vibration results.

INTRODUCTION

Historically, the *in vivo* study of basal cochlear mechanics was limited to measurements of the basilar membrane (BM). The advent of optical coherence tomography (OCT) in the last decade has allowed for vibrometry at a depth, facilitating the study of intra-organ of Corti complex (OCC) motions. Of particular interest is the motion of the electromotile outer hair cells (OHCs), which play an important role in amplifying vibration responses and improving the range of sound-pressure levels (SPLs) over which hearing operates.

Several issues complicate the interpretation of OCT measurements. Firstly, the motion of the OHC region is not uniform. The OHCs are 40 μm long and 10 μm wide, and come in rows of three per longitudinal cross-section. The apical surface of the OHCs, called the reticular lamina (RL), moves differently from the basal surface attached to the Deiters' cells as the OHC compresses and expands due to electromotility [1]. Moreover, the OHCs within a row move differently from each other [2].

A second complication is that measurements are generally taken at an angle with respect to the transverse anatomical orientation of the cochlea, and this angle is not known *a priori*. This introduces two ambiguities: (1) displacements measured via OCT are projections of the three-dimensional motion onto an unknown axis, and (2) measured points at the OHC and BM within a single optical axis measurement (A-scan) will in general lie in different longitudinal cross-sections. The first of these ambiguities was discussed by Cooper et al [3]. Their measurements showed that the phase difference between OHC and BM motion relied heavily on the viewing angle. The second of these ambiguities was discussed by Frost et al [4], wherein we developed a program that measured the relative anatomical distances between structures imaged with OCT. We used this program to measure displacement of the OHC and BM at the same cross-section, and showed that this correction revealed up to 1/4 cycle difference in OHC-BM displacement phase when displacement-accounted (single cross-section) results were compared to single-measurement (two different cross-section) results.

With these complications in mind, it is difficult to fully interpret OCT measurements of OHC displacement that are reported without the viewing angle specified. The group of Ren has achieved BM and OHC-region displacement measurements taken at a purely transverse angle, thus measuring purely transverse motion in a single tonotopic cross section, both in gerbil and mouse [5, 6]. The instrument they use is similar to

OCT, but does not provide imaging. The OHC-region measurement was reasoned to be the RL, but this identification is not ironclad. They found that RL displacement phase led BM at low frequencies, and this lead decreased monotonically until the structures were in phase at about 0.8 of the best frequency (BF). After this zero crossing, the RL re BM phase continued its monotonic decrease, with the RL lagging the BM at near- and supra-BF frequencies. Our displacement-accounted data of OHC-region and BM in the same tonotopic cross-section taken at a viewing angle with a significant longitudinal component found a phase difference of a different character. OHC led BM across frequency, including at high frequencies – where Ren et al saw an 80°*lag*, we saw a 90°*lead*. Given the ambiguities and technical variations noted above, the difference in observations is not surprising.

In order to address the experimental variations and ambiguities, and thereby enhance the value of intra-OCC motion measurements, we have developed a method to isolate the transverse and longitudinal components of motion of structures within the OCC, wherein we account both for the longitudinal distance between structures and the projection incurred by the viewing angle. Similar to the work of Lee et al, we do so by taking measurements at multiple viewing angles [7]. Our method requires no *a priori* knowledge of either measurement angle, or of the positions of the structures being measured. We determine a linear approximation of the longitudinal direction at acquisition time, followed by *post hoc* registration of structures measured at several longitudinal locations and two viewing angles. We then analyze the measured displacements to achieve a reconstructed longitudinal-transverse profile of a structure's motion.

We present the method, an analysis of its fidelity with respect to viewing angle, and *in vivo* data from the base of the gerbil cochlea in which the longitudinal-transverse motion at the basal region of several OHCs has been reconstructed. In this sample data set, the phase of our reconstructed transverse displacements were similar to the pure-transverse RL displacements measured by Ren. Also, the magnitude of longitudinal (base-to-apex) OHC displacement was generally smaller than that of transverse OHC displacement and $\sim$ 180°out of phase with transverse (towards scala vestibuli) OHC displacement, across frequency.

METHODS

Acquisition

The acquisition process follows a few steps: (1) prior to acquisition, ensure the BM looks as horizontal as possible in two orienting B-Scans, (2) use these B-scans to determine the approximate longitudinal direction, (3) decide on a structure-category of interest (for example, base of the OHC) and take A-scan displacement measurements including that structure-category at multiple longitudinal locations, (4) rotate the preparation and again find two new orienting B-scans with the BM appearing horizontal, (5) again, find the approximate longitudinal direction and take A-scan measurements of the same structure-category of interest at multiple longitudinal locations.

Orienting the preparation so that the BM appears horizontal in each cross-section ensures that the radial component of the optic axis is approximately zero. This simplifies the problem to two dimensions – transverse and longitudinal.

Determining the approximate longitudinal direction works via a linear approximation of the cochlea's anatomical coordinates, similar to the planar approximation we employed in [4]. As we only need the longitudinal direction for acquisition, this is a simpler process – we use ThorImage (the imaging program of the Thorlabs Telesto OCT) and locate a landmark in our orienting B-scans; in the example in Fig. 1 we use the thickest part of the BM. We record the optical coordinates at this position in the two B-scans, $p_1 = (x_1, y_1, z_1)$ and $p_2 = (x_2, y_2, z_2)$. The difference between these points is a linear approximation of a vector in the longitudinal direction, so the unit longitudinal vector is

$$l = \frac{p_2 - p_1}{|p_2 - p_1|}. \tag{1}$$

This process is illustrated in panels A and B of Fig. 1.

We can find points of measurement for some structure of interest, say the base of the OHC, at fixed increments along the longitudinal direction. If we start at a point q_0 containing that structure, and want to

measure N points over longitudinal distance L, we measure at

$$q_n = q_0 + \frac{nL}{N} l,\ n = 0, 1, \ldots, N-1. \tag{2}$$

This is illustrated in panel C of Fig. 1. Note that q_0 need not be one of p_1 or p_2; in this example p_1 and p_2 are within the BM and the q positions are at the base of the OHCs.

We take volume scans after each run so that outside of the time pressure of an experiment, we can apply our more complex orientation program [4]. In doing so, we can assess the accuracy of our assumption that the radial component of our measurement axis is 0, as well as the direction of the longitudinal vector.

Registration

As we have made sure to remove the radial component of motion from our measurements, we can assume the optical z axis is comprised of only longitudinal (l) and transverse (t) components. We write the optical axis' unit vector as a two-dimensional vector in anatomical coordinates, $z = (z_l, z_t)$.

Eqn. 1 is used in the acquisition step to find the longitudinal vector l, which has optical x, y and z components. The z component of this vector represents the amount of longitudinal motion that is projected onto the optical axis, z_l. To find the t component of z, we need only to recall that z is a unit vector, so that $z_l^2 + z_t^2 = 1$. Using the notation from Eqn. 1, we have

$$z_l = \frac{z_2 - z_1}{|p_2 - p_1|}, \tag{3}$$

$$z_t = \sqrt{1 - z_l^2}. \tag{4}$$

This is illustrated in panel C of Fig. 1.

Knowing this, we can relate the OHC and BM longitudinal locations within a single measurement. If the structures along a single measurement axis are spaced Δz apart, then the OHCs lie $\Delta l = z_l \Delta z$ apical of the BM. The measured BM Δl apical of this measurement is thereby in the same longitudinal cross-section as the OHC in the first measurement. We call these BM and OHC measurements *aligned* to one another. At each measurement angle, we compose a list of all aligned OHC and BM measurements. This process is illustrated in panels D and E of Fig. 1.

To register points to one another between viewing angles, we use the phase of BM motion. By matching the phase responses of BM measurements taken at different viewing angles, we can register the cross-sections in which these BM motions were measured. This operates under the assumption that BM motion is entirely transverse, so that its phase response at each cross-section will be the same at each viewing angle. Having registered BM points to one another, we can then consult our list of aligned BM-OHC pairs. The OHCs aligned to registered BM positions are also registered, allowing us to isolate the same OHCs at different viewing angles.

Reconstruction

Each OCT measurement is a projection of a true 3-D motion onto the optical z axis. In the current context, we have made efforts to eliminate the representation of radial motion in our projection, so that the problem can be framed as the projection of a 2-D longitudinal-transverse *true motion* d onto a 2-D transverse-longitudinal z axis, forming the *projected motion* δ.

Above we described the method by which we determine the z_l and z_t components of the optical axis in each experiment. The projection onto this axis is given by the dot product

$$\delta = z \cdot d = \begin{pmatrix} z_l & z_t \end{pmatrix} \begin{pmatrix} d_l \\ d_t \end{pmatrix}. \tag{5}$$

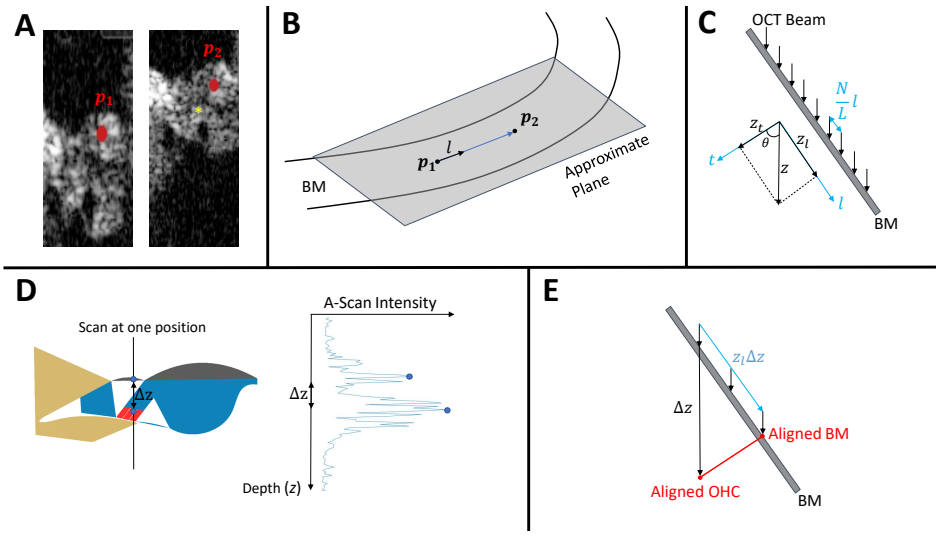

FIGURE 1. A – Two parallel B-Scans from a single volume, about 50 μm apart, on which we have marked points p_1 and p_2 used to determine the longitudinal direction l. We have selected the landmark to be the BM at its widest point. We have ensured that the BM appears approximately horizontal in each B-Scan, so as to remove radial displacement contributions. Included also is a yellow star at the OHC base, which could be used as q_0 to measure OHC base at multiple longituinal cross-sections once the l direction has been determined. **B** – A cartoon of the BM, with true longitudinal axis varying in space. We have approximated this axis by a line passing through both p_1 and p_2. **C** – A cartoon of the BM projected onto the longitudinal-transverse plane, in which our A-Scans lie. We take A-Scans along the z axis at multiple evenly spaced longitudinal positions. We can determine the anatomical components of the z vector via geometry, knowing l and knowing that z has unit length. **D** – A cartoon of the organ of Corti complex and an experimentally acquired A-Scan. We measure the distance between OHC base and BM in the A-Scan, Δz, to determine the longitudinal displacement between these structures. Gray is the BM, with the fluid compartment scala tympani above. Blue is the organ of Corti with red the OHCs. Tan is the spiral limbus and tectorial membrane. Scala vestibuli is the fluid compartment below to OCC. **E** – A cartoon of the BM in the longitudinal-transverse plane similar to **C**. The OHC at a measurement position is $z_l\Delta z$ apical of the BM at that same position. This OHC's *aligned* BM point is that which is measured at this same longitudinal position.

At each angle, if we are truly measuring at one position, d will remain the same and z will change. If we take measurements at two angles, we form the system of equations:

$$\begin{pmatrix}\delta_1\\ \delta_2\end{pmatrix} = \begin{pmatrix}l_1 & t_1\\ l_2 & t_2\end{pmatrix}\begin{pmatrix}d_l\\ d_t\end{pmatrix}, \tag{6}$$

where the rows of the matrix are the z axes corresponding to each angle, and δ_i is the projection measured at the i^{th} angle.

We measure δ_i and determine the l and t components of the z axis as described above. We want to reconstruct d, which can be done by inverting the matrix in Equation 6. This is possible if and only if the rows of the matrix are linearly independent, i.e. if the measurement axes are not colinear. As long as we measure at two sufficiently distinct (to be quantified shortly) angles, we can reconstruct d by performing the matrix inverse:

$$\begin{pmatrix}d_l\\ d_t\end{pmatrix} = \frac{1}{l_1t_2 - l_2t_1}\begin{pmatrix}t_2 & -t_1\\ -l_2 & l_1\end{pmatrix}\begin{pmatrix}\delta_1\\ \delta_2\end{pmatrix}. \tag{7}$$

Achieving measurements of the same structures at different angles is constrained by the preparation. In practice, a 15 degree rotation is tractable in our preparation, but significantly larger angles are not consistently achievable. The precision of our reconstruction can be found via the *condition number* κ of our projection matrix in Eqn. 6. The condition number is defined as

$$\kappa(A) = \frac{|\sigma_{max}|}{|\sigma_{min}|}, \tag{8}$$

Angular deviation	Condition number κ
20°	5.67
15°	7.60
10°	11.43
5°	22.90
1°	114.59

TABLE I. A table of condition numbers for the projection matrix at possible measurement angular deviations.

where σ_{max} and σ_{min} are the maximum and minimum singular values (similar to eigenvalues) of a given matrix A. The condition number of a matrix represents how "well-posed" a system of equations is, i.e. how close to singular the matrix is. A matrix with a large condition number will amplify noise significantly more than a matrix with a small condition number. The "rule of thumb" is that SNR is reduced by a factor of about κ. Note that a matrix and its inverse have the same condition number.

Table I shows condition numbers for some possible angular deviations. Condition number does not depend on the absolute angle, but only the absolute difference between the two measurement angles. Our usual precision is on the order of 0.1 nm, and our signal at higher dB SPL is in the range of 1-10 nm. The realized 15-degree angle will lead to an eight-fold increase in the noise level, which means our results are accurate to about 0.8 nm.

RESULTS

We have employed the method described above in the base of the gerbil cochlea, with measurements taken through the round window membrane at angles of approximately 45° and 60° relative to the transverse direction. Going from one to the other angle was accomplished with a goniometer that serves as the head-holder. The base of the OHC was used as the structure of interest. Using the ThorImage positioning system and the method outlined above, we took data at 11 positions spaced 15 μm apart longitudinally. We stimulated the ear with one-second, 15-frequency multitone stimuli at 80 dB SPL. We did this at both angles.

As we stepped longitudinally along the cochlea, we expected to see the phase response at the BM vary along with the tonotopic cross-section. This behavior is displayed in Fig. 2, providing evidence that our acquisition method is truly stepping along the tonotopic axis.

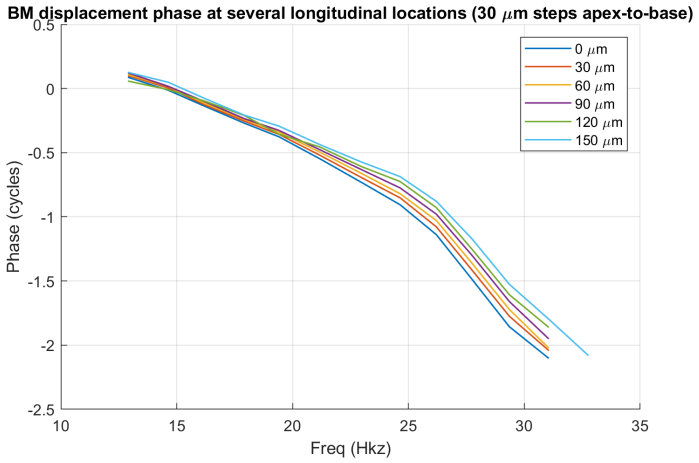

FIGURE 2. Phase of BM displacement measured in response to 80 dB SPL 15-frequency multitone stimulus, taken at several points along the longitudinal axis of the cochlea. The OCT beam is oriented at 45° to the BM, and we have stepped 15 μm at a time along the cochlea over a 150 μm range. We display every other step here to make clear the travelling wave pattern of the displacement as we step from apex to base.

As for the registration process, Fig. 3 shows matched BM phases taken at two different angles. We did not know the overlap of the measured regions at each angle *a priori* and we found a 60 μm region of longitudinal overlap *post hoc*, five positions spaced by 15 μm. Two of these matched positions are shown; these two were spaced by 45 μm.

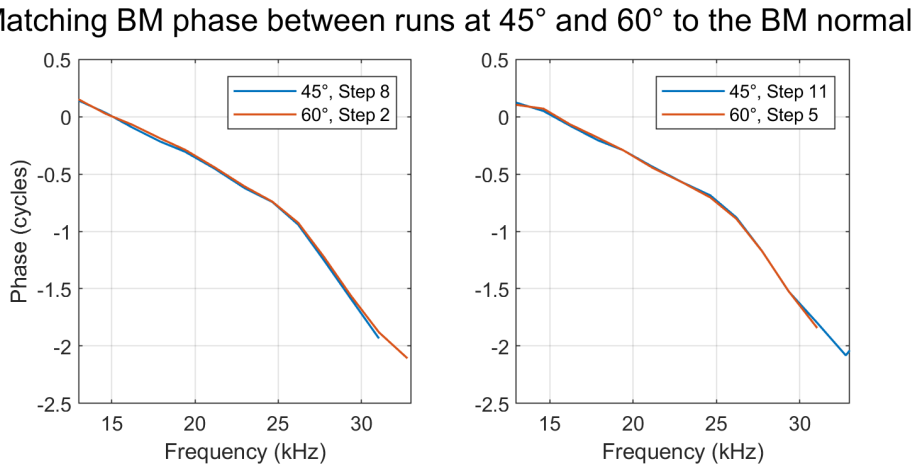

FIGURE 3. Matched BM phase plots used for registering locations between measurement angles. Phase was matched at five positions; two are shown. Each "step" was measured 15 μm basal of the previous step, and these two subplots show positions 45 μm apart from one another, with the panel on the right basal of that on the left.

Applying our reconstruction method to the associated aligned OHCs we arrive at the two-dimensional frequency responses presented in Fig. 4. At all five registered locations (two are shown), transverse OHC motion was significantly larger than longitudinal OHC motion across the bulk of the frequency range at 80 dB SPL. Reconstructed transverse OHC displacement phase underwent the linear lead-to-lag transition measured by Ren and colleagues, with zero-crossing near 0.8BF [5, 6].

The longitudinal displacement phase led transverse displacement phase by ∼180°. (Recall the transverse axis points toward scala vestibuli, the longitudinal axis points toward the base.) With respect to our coordinate system, this means that towards-scala tympani transverse displacement is approximately in phase with basal-to-apical longitudinal displacement.

CONCLUSION

We have developed and presented the application of a method by which longitudinal-transverse 2-D intra-OCC displacements can be reconstructed from 1-D OCT measurements taken at two measurement angles, without any *a priori* knowledge of the measurement angles or measurement locations. We have presented the application of this method to reconstructing the motion of the base of OHCs across a 45 μm longitudinal region of the base of the cochlea. This method can be used to reconstruct the 2-D motion of any structure in the OCC. Measurements of this type help to resolve apparent discrepancies between groups, contextualize 1-D measurements and serve as a step towards the goal of reconstructing total 3-D intra-OCC displacements.

A 2-D understanding of intra-OCC motions provides significantly more information about the mechanical operations than single-dimensional measurements. In particular, 1-D measurements of relative BM-OHC displacement phase taken with a large longitudinal component, even when the longitudinal distance between the structures was accounted for, did not show the ∼0.8 BF lead-to-lag transition of transverse OHC phase re BM that was observed when measuring purely transverse motion, as seen both in our reconstruction and in [5]. As 0.8 BF is approximately the onset frequency of BM displacement nonlinearity, this transition may be key for understanding the operation of the cochlear amplifier. This is one example of the significant features of motion that are revealed by multi-dimensional measurements of OCC vibration.

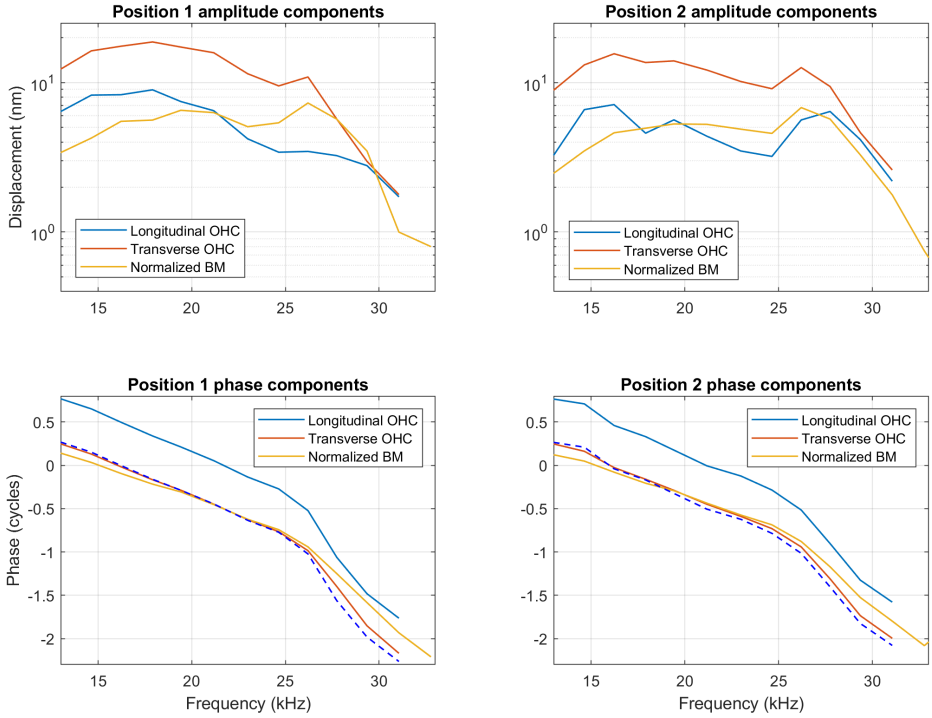

FIGURE 4. Amplitude and phase response of transverse and longitudinal OHC motion, reconstructed at two different positions spaced 45 μm apart longitudinally. Presented also is the BM displacement at this position, taken from the aligned BM displacement with 45° measurement angle. We have normalized this BM displacement value by multiplying by $\sqrt{2}$ – the theoretical geometric loss incurred by measuring a purely transverse BM motion at a 45° angle. The dashed blue phase curve is the longitudinal OHC phase curve subtracted by 180°, i.e. the apex-to-base phase.

REFERENCES

1. J. B. Dewey, A. Altoe, C. A. Shera, B. E. Applegate, and J. S. Oghalai, "Cochlear outer hair cell electromotility enhances organ of corti motion on a cycle-by-cycle basis at high frequencies in vivo," Proceedings of the National Academy of Sciences of the United States of America **118**, 37625 (2021).
2. N. H. Cho and S. Puria, "Motion of the cochlear reticular lamina varies radially across outer-hair-cell rows," bioRxiv (2022), 10.1101/2022.03.01.482580, https://www.biorxiv.org/content/early/2022/03/04/2022.03.01.482580.full.pdf.
3. N. P. Cooper, A. Vavakou, and M. van der Heijden, "Vibration hotspots reveal longitudinal funneling of sound-evoked motion in the mammalian cochlea," Nature Communications **9**, 3054 (2018).
4. B. L. Frost, C. E. Strimbu, and E. S. Olson, "Using volumetric optical coherence tomography to achieve spatially resolved organ of corti vibration measurements," Journal of the Acoustical Society of America **151**, 1115–1125 (2022).
5. W. He and T. Ren, "Transverse vibrations of the reticular lamina and basilar membrane in the basal turn of gerbil cochleae," (2022), association for Research in Otolaryngology Midwinter Meeting.
6. T. Ren, W. He, and D. Kemp, "Reticular lamina and basilar membrane vibrations in living mouse cochleae," Proceedings of the National Academy of Sciences of the United States of America **113**, 9910–9915 (2016).
7. H. Y. Lee, P. D. Raphael, A. Xia, J. Kim, N. Grillet, B. E. Applegate, A. K. E. Bowden, and J. S. Oghalai, "Two-dimensional cochlear micromechanics measured in vivo demonstrate radial tuning within the mouse organ of corti," Journal of Neuroscience **36**, 8160–8173 (2016).